Tectonophysics 464 (2009) 70–83

Contents lists available at ScienceDirect

Tectonophysics

journal homepage: www.elsevier.com/locate/tecto

The three-dimensional thermo-mechanical signature of ridge subduction and slab window migration

Wesley G. Groome *, Derek J. Thorkelson [1]

Department of Earth Sciences, Simon Fraser University, 8888 University Dr. Burnaby, BC, Canada

ARTICLE INFO

Article history:
Received 18 April 2007
Received in revised form 21 June 2008
Accepted 3 July 2008
Available online 12 July 2008

Keywords:
Slab windows
Ridge subduction
Three-dimensional numerical models
Deformation kinematics
Metamorphism
Topographic uplift

ABSTRACT

We present a series of three-dimensional numerical models investigating possible thermal and mechanical effects of ridge subduction and slab window migration. Ridge subduction is a fundamental process of plate tectonics, and the geologic manifestations in the overriding lithosphere have been investigated in many convergent margin settings. Many of the geologic effects of slab window migration (e.g., anomalous high-*T* metamorphism in the forearc, non-arc-like magmatism in the volcanic arc) are explained primarily by the introduction of a region of hot, upwelling asthenospheric mantle in the subduction zone environment. Using end-member boundary conditions and idealized geometries, our models address the thermal and corresponding mechanical manifestations of slab window migration, and our results provide a general agreement with observations from interpreted regions of slab window migration. Our models show that protracted heating in the forearc region should result in protracted high-temperature metamorphism, associated rheologic weakening and strain partitioning and changes in the topographic uplift pattern in regions affected by slab window migration. Although these models are idealized, they do provide valuable insight into the geodynamics of slab window environments and provide a valuable starting point for further exploration.

1. Introduction

Ridge subduction is an inevitable consequence of plate tectonics that significantly affects the margin of the overriding plate. Ridge subduction leads to the formation of a slab window, in which hot asthenospheric mantle wells up in the gap created between the two diverging plates (e.g., Marshak and Karig, 1977; Delong et al., 1979; Dickinson and Snyder, 1979; Forsythe and Nelson, 1985; Thorkelson and Taylor, 1989; Sisson and Pavlis, 1993; Thorkelson, 1996). The exact geometry and geodynamic effects of ridge subduction and slab window migration depend primarily on the geometry of the ridge being subducted (i.e., the orientation of the ridge relative to the overriding plate, the arrangement of ridge and transform fault segments, etc., cf., Thorkelson, 1996). However, regardless of the specific geometry of a given slab window, there are several common geologic manifestations related to slab window migration, including anomalous high-*T* metamorphism in the forearc region (e.g., Delong et al., 1979; Underwood et al., 1993; Sisson and Pavlis, 1993; Brown, 1998; Groome et al., 2003), non-arc-like volcanism in the volcanic arc (e.g., Johnston and Thorkelson, 1997; Breitsprecher et al., 2003; Madsen et al., 2005), rapid changes in deformation style on either side of the slab window (e.g., Cembrano et al., 2002; Haeussler et al., 2003) and enhanced topographic uplift rates above the slab window (e.g., Buiter et al., 2002; Rogers et al., 2002; Legabrielle et al., 2004; Espinoza et al., 2005), all of which are, in part, a manifestation of the replacement of cold, dense subducting lithosphere with hot, buoyant asthenospheric mantle in the slab window.

The geologic consequences of ridge subduction have been investigated in many convergent margin settings, including the North American Cordillera (e.g., Thorkelson and Taylor, 1989; Barker et al., 1992; Sisson and Pavlis, 1993; Breitsprecher et al., 2003; Groome et al., 2003; Sisson et al., 2003), Central America (e.g., Johnston and Thorkelson, 1997; Rogers et al., 2002), the Patagonian Andes (e.g., Suarez et al., 2000; Legabrielle et al., 2004, Espinoza et al., 2005), the Antarctic Peninsula (e.g., Barker, 1982) and Japan (e.g., Hibbard et al., 1993; Underwood et al., 1993; Brown, 1998; Iwamora, 2000). Some of the forearc geologic features that have been attributed to ridge subduction include: 1) anomalous magmatism and related high-temperature metamorphism, including in the accretionary prism (e.g. Barker et al., 1992; Underwood et al., 1993; Sisson and Pavlis, 1993; Groome et al., 2003; Pavlis and Sisson, 2003); 2) elevated uplift rates in the forearc and arc regions (e.g. Rogers et al., 2002; Espinoza et al., 2005); and 3) changes in structural style on either side of the slab window (e.g. Pavlis and Sisson, 2003; Legabrielle et al., 2004) (Fig. 1).

The forearc region is typically a setting for low-temperature (+/− high-pressure) metamorphism resulting from low geothermal gradients due to the subduction of cold oceanic lithosphere (e.g., Turcotte

* Corresponding author. Present Address: Newcrest Mining Ltd. Orange, NSW, Australia. Fax: +61 1 604 291 4198.
E-mail address: Wesley.groome@newcrest.com.au (W.G. Groome).
[1] Fax: +61 1 604 291 4198.

0040-1951/$ – see front matter
doi:10.1016/j.tecto.2008.07.003

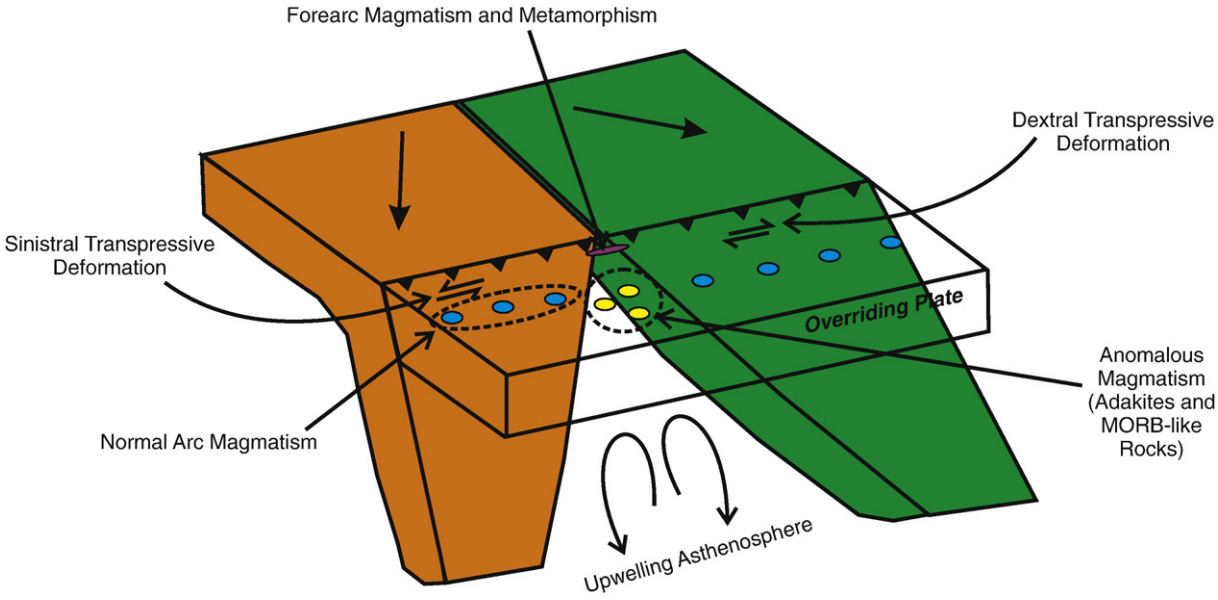

Fig. 1. Schematic block diagram of the key features of slab window environments. Modified from Johnston and Thorkelson (1997). The environment shown here has symmetrically-spreading downgoing plates (in orange and green) with a symmetric zone of upwelling asthenosphere in the slab window. There is no thermal erosion along the trailing edge of either plate. Note that on either side of the slab window, the sense of transpressional deformation in the forearc region changes due to changing boundary configurations (i.e. differing senses of oblique convergence between the downgoing and overriding plates). The change in dip between the two plates is schematic and not reflective of any fundamental features of slab windows. Arrows on the subducting plates denote the relative convergence between each plate and the overriding plate. (For interpretation of the references to color in this figure legend, the reader is referred to the web version of this article.)

and Schubert, 2002). Geothermal gradients increase laterally away from the forearc region, towards the arc and backarc, as a result of thermal relaxation in the overriding lithosphere and the advection of hot asthenosphere in the mantle wedge (e.g., Turcotte and Schubert, 2002). This situation should result in lateral gradients in metamorphism from forearc to backarc that ideally should go from low-temperature (+/− high-pressure) metamorphism in the forearc, Barrovian-type metamorphism in the region between the arc and forearc, and high-temperature, low-pressure style metamorphism in the arc and backarc region (e.g., Bucher and Frey, 1994). However, late Mesozoic/early Cenozoic metamorphism in the forearc region of the northern Cordillera (British Columbia and Alaska) is unusually high temperature, including andalusite- and sillimanite-grade metamorphism (e.g., Sisson and Pavlis, 1993; Groome et al., 2003; Pavlis and Sisson, 2003) and accompanied by mafic to felsic magmatism with geochemical signatures suggesting an asthenospheric mantle contribution (e.g., Barker et al., 1992; Sisson et al., 2003; Groome et al., 2003; Madsen et al., 2005). These features have been attributed to the subduction of various spreading ridges beneath the forearc region, resulting in the juxtaposition of hot asthenospheric mantle at the base of thin forearc lithosphere (e.g., Barker et al., 1992; Sisson and Pavlis, 1993; Groome et al., 2003; Madsen et al., 2005).

Uplift of the forearc region occurs when a spreading ridge begins to subduct because the ridge is a topographic high and is positively buoyant, so there is resistance to subduction, leading to a change in the velocity field in both the subducting and overriding plates resulting in contraction and uplift in the overriding forearc, similar to what is seen in regions of seamount subduction (e.g., Dominguez et al., 2000). Farther inboard, broad uplift above subducting spreading ridges has been recognized in Central America (e.g., Rogers et al., 2002) and above regions of lithosphere break-off in the Carpathian region (e.g., Wortel and Spakman, 2000) where asthenospheric mantle replaces lithospheric mantle. The replacement of relatively cool lithospheric mantle by relatively hot asthenospheric mantle changes the isostatic balance of that region because the hot asthenosphere is less dense than the lithosphere it replaces, leading to elevated vertical velocities above the zone of asthenospheric upwelling.

Finally, changes in deformation style as a slab window migrates result from changes in plate convergence vectors on either side of the slab window (e.g., Suarez et al., 2000; Bradley et al., 2003; Pavlis and Sisson, 2003; Legabrielle et al., 2004; Espinoza et al., 2005). The change in deformation in the overriding lithosphere is largely a function of the change in convergence orientation and velocity on either side of the slab window. As an example, if ridge subduction is orthogonal to the subduction zone, the two plates must be diverging with different senses of transpressive motion in the overriding plate (e.g., Thorkelson, 1996). This means that on one side of the slab window, deformation in the overriding lithosphere should record transpressive deformation with a different sense of shear as the other side of the slab window. Immediately above the slab window, the velocity vectors should be divergent, and may lead to the development of extensional structures. However, if both plates are transpressive in the same direction, but with different amounts of subduction zone-parallel plate motion, the amount of transpressive deformation in the overriding lithosphere will change as the slab window migrates.

In this paper, we use simplified three-dimensional numerical experiments to explore some of these assertions about the thermal and mechanical consequences of ridge subduction and slab window formation. First, we present a thermal model illustrating the effects of a migrating slab window on the thermal evolution of the overriding lithosphere with emphasis on the forearc region. We then use this model to constrain a mechanical model investigating the effects of thermal weakening resulting from slab window migration. While our models are first pass attempts at modeling the geodynamics of slab window environments, the results generally support many of the assertions presented above, and provide new insight into the possible effects slab windows have on orogenic evolution.

2. Model set-up

The model presented here (Fig. 2) consists of a lithospheric block with dimensions of 1000 km (*Y*) by 600 km (*X*) by 100 km (*Z*) containing a gently-dipping subducting oceanic lithosphere, an overriding lithosphere with properties consistent with continental lithosphere and a

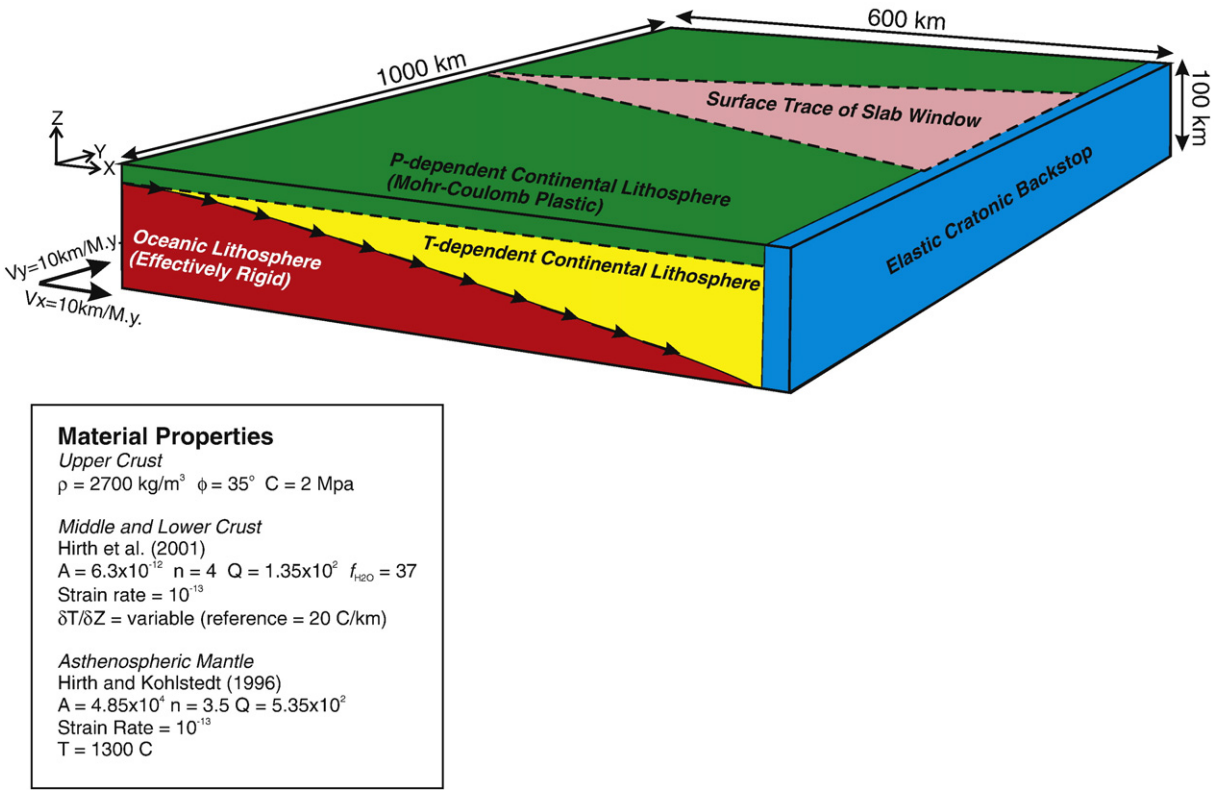

Fig. 2. Schematic block model of the numerical experiments presented in this paper showing the mechanical layering, model dimensions and the location of the slab window. The material properties used in the model are also listed on the figure. The model environment is 600×1000×100 km. Due to boundary effects, the model results shown in this paper are restricted to the zone 300–600 km from the elastic backstop.

far-field elastic backstop representing a cratonic margin, similar to existing models of subduction zones (e.g., Koons, 1990; Willett et al., 1993; Beaumont et al., 1996; Ellis and Beaumont, 1999; Koons et al., 2002; Upton et al., 2003). The subducting oceanic lithosphere contains a spreading ridge that intersects the subduction zone orthogonally, resulting in the formation of a simple symmetric slab window (e.g., Thorkelson, 1996). This slab window is a zone of hot asthenospheric upwelling surrounded by cooler, normal subducting lithosphere.

For simplicity, and to act as a starting point for future investigation, we use a single kinematic condition of orthogonal plate convergence in the mechanical model ($V_x = V_{total} = 10$ km/my). For the thermal model, we use a kinematic condition where the triple junction, and resulting slab window, migrates parallel to the plate boundary at a rate of 10 km/my. The slab window in these models is treated as a discrete domain of hot, weak material within the downgoing plate that moves at the same velocity and in the same direction as the material on either side of it. In this case, the window maintains a constant size and shape through time, reflecting a stable plate configuration in which plate divergence is uniform through time. This construction was done for numerical stability in the modeling environment and represents a simplification of the natural case in which the slab window will grow and change shape through time as the two diverging plates continue to diverge and thermal erosion occurs along the trailing edges of the subducting plates. Convergent velocities in our models are at the low end of those encountered on Earth and thus provide estimates for the maximum amount of heating related to slab window migration (i.e., slow convergence = maximum heating times).

The following model assumptions and simplifications are made 1) heat transfer through the overriding lithosphere is by conduction alone, 2) the slab window has a constant temperature equal to the temperature of the upwelling asthenosphere (~1300 °C) (e.g., Hirth and Kohlstedt, 1996), 3) the ductile portion of the overriding lithosphere is governed by the wet-quartzite flow law of Hirth et al. (2001), 4) weakening of the overriding lithosphere is only by thermal processes (i.e., weakening associated with strain localization, partial melting or metamorphic weakening is disregarded), 5) erosion does not occur, 6) the slab window maintains a simple geometry, and 7) density is uniform through the model and velocity boundary conditions are kinematically defined.

Assumption (1) is considered valid because we have no constraints on advective heat transfer through the overriding lithosphere via processes such as hydrothermal fluid flow or magmatic transfer, therefore we do not wish to impose an arbitrary advective regime. Assumption (2) is considered valid because upwelling asthenospheric mantle should advect heat faster than it looses heat via conduction into the surrounding lithosphere, at least at the locus of upwelling. We chose to use a wet-quartzite flow law to constrain the flow strength of the lithosphere in our model. Due to the uncertainties of constraining the flow strength of the ductile lithosphere, we consider this to be a valid starting point and have not pursued a sensitivity analysis related to changes in material properties of the lithosphere as a whole, although analytical treatments suggest that the differences in flow strength at high temperatures between plagioclase-dominated materials is minimal and significant changes in flow strength occurs at low temperatures (e.g., Ji and Zhao, 1993; Ji and Xia, 2002). Assumptions (5) and (6) are also made because we do not wish to impose an arbitrary erosion regime or slab window geometry, although these may significantly alter the model results. Finally, assumption (7) is

Fig. 3. A: Map view, B: Cross-sections of the thermal structure perpendicular to the plate margin and C: thermal histories 50, 150 and 250 km from the plate margin. The cross-sections show the instantaneous thermal structure of the model at a time when the slab window is in the middle of the model domain. The thermal histories display the histories at various depths from the start (0 my) to the finish (30 my) of the model. The locations of the thermal histories are indicated on the map by points 1, 2 and 3. Arrow 1 shows the time when the leading edge of the slab window encounters the section line and arrow 2 shows the time when the centre of the slab window is in the section line.

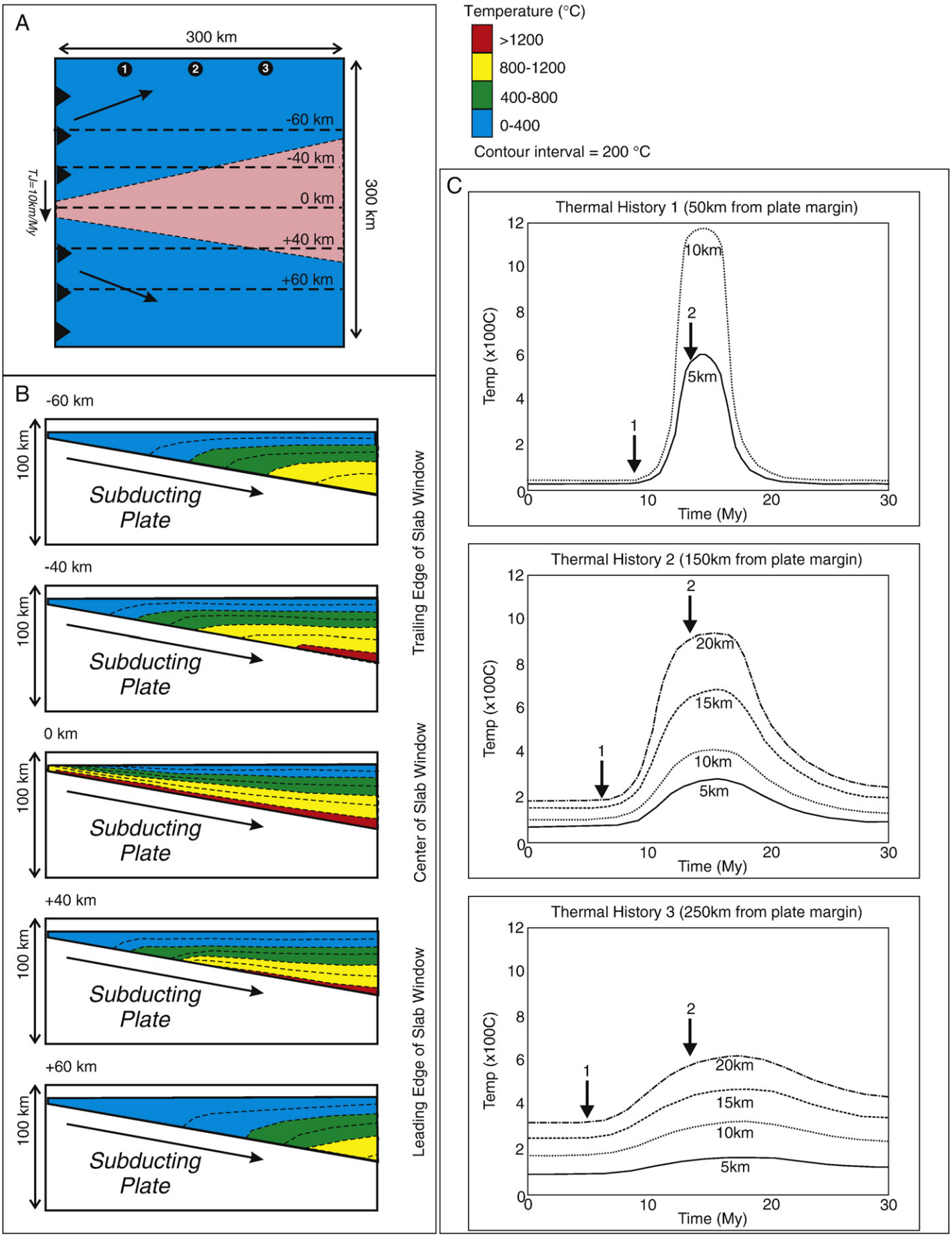
A
300 km
1
2
3
-60 km
-40 km
0 km
+40 km
+60 km
300 km
T-F=10km/My
Temperature (°C)
>1200
800-1200
400-800
0-400
Contour interval = 200 °C
B
-60 km
100 km
Subducting Plate
-40 km
0 km
+40 km
+60 km
Trailing Edge of Slab Window
Center of Slab Window
Leading Edge of Slab Window
C
Thermal History 1 (50km from plate margin)
Temp (x100C)
Time (My)
10km
5km
Thermal History 2 (150km from plate margin)
20km
15km
10km
5km
Thermal History 3 (250km from plate margin)
20km
15km
10km
5km

made for simplicity because we impose a velocity boundary condition to drive subduction, therefore do not need to appeal to a particular density structure. Although we don't consider many of the above factors in our numerical models, we do qualitatively address their potential effects in the discussion.

3. Model environment and constitutive relationships

The thee-dimensional models are generated using the numerical code FLAC^{3D} (Itasca, 2005), which has been modified to accommodate large strains (e.g., Koons et al., 2002; Upton et al., 2003; Johnson et al., 2004; Groome et al., 2008). Materials in the model are represented by polyhedral elements with a three-dimensional grid using an explicit time-marching solution with a form of dynamic relaxation. Mechanical responses of each element follows a prescribed linear or non-linear stress–strain law in response to applied forces or kinematic boundary conditions and thermal responses of each element follows a conductive heat transfer relationship that relates thermal diffusivity and proximity to a heat source.

The models are not coupled thermo-mechanical solutions; rather, they are results of a purely thermal model are used to constrain the mechanical conditions in a purely mechanical solution. Thermal model results provide information about the temperature distribution in the model domain. The initial thermal state of the model is determined by applying a constant heat source at the base of the lithosphere (1300 °C), fixing the temperature at the surface to be 0 °C and fixing the temperature of the subducting slab in accordance with analytical treatments of Turcotte and Schubert (2002) and allowing the model to thermally equilibrate via conductive heat transfer. Furthermore, no internal source of heat is described in either lithospheric plate.

4. Model description and assumptions

4.1. Thermal

In the initial condition of our models, the temperatures in the overriding lithosphere are warm relative to those found in natural, steady-state subduction systems where old, cold slabs are being subducted (e.g., Turcotte and Schubert, 2002). We consider the elevated temperatures in our model to be appropriate because in a slab window environment, the subducting plate is relatively young and therefore not 'old and cold' as expected in many subduction settings. In the models presented here, we are more interested in the pattern of heating and cooling related to slab window migration, rather than absolute temperatures, and thus consider the elevated initial temperatures to be non-critical.

After the problem domain thermally equilibrates by conductive heat transfer, a slab window is placed at the base of the overriding plate. The slab window is defined as having a uniform temperature of 1300 °C, which results in the transfer of heat to the relatively cool overriding lithosphere as a function of the proximity to the heat source described by:

$$\frac{\partial T}{\partial t} = \kappa \nabla^2 T \tag{1}$$

where $\frac{\partial T}{\partial t}$ describes the time-dependent temperature of a point, κ is the thermal diffusivity and the final term describes the proximity to the heat source in three dimensions. The size of the slab window is arbitrarily chosen as 10 km wide (one cell in the model) at the point of subduction and widens at depth to a width of 200 km at a depth of 100 km. The shape of the window is maintained as a single triangle for simplicity of modeling. The entire region within the triangular slab window is kept at a constant temperature of 1300 °C, equivalent to the upwelling asthenosphere, and the thermal structure is allowed to decay along strike in both directions as a function of conductive heating and cooling. Above the slab window, in the overriding plate, temperatures are free to respond in a conductive manner as a function of proximity to the hot slab window, as described in Eq. (1). In the models with a migrating slab window, the slab window migrates parallel with the plate margin at a fixed velocity (10 km/my) and regions along the leading edge of the hot slab window will heat up, and regions along the trailing edge will cool as governed by the relationship:

$$\frac{\partial T}{\partial t} = \kappa \nabla^2 T + U \nabla T \tag{2}$$

where U is the migration velocity of the slab window.

4.2. Mechanical

Mechanical model results provide information about the velocity, displacement and strain fields within the problem domain and we present the results in terms of strain rate and velocity. The model domain is mechanically layered with an upper crust described by a pressure-dependent plasticity constitutive relationship (Mohr–Coulomb) and a lower crust described by a temperature-dependent plasticity constitutive relationship (Drucker–Prager) constrained by empirical flow law data for wet quartzite (Hirth et al., 2001). The pressure-dependent strength of the upper crust is based on the Mohr–Coulomb constitutive relationship:

$$\sigma_c = \sigma_n \tan\phi + C \tag{3}$$

where σ_c is the failure shear stress (MPa), σ_n is the normal stress (ρgh) (MPa), ϕ is the internal angle of friction and C is cohesion (MPa) (all of these parameters are listed on Fig. 2). The temperature-dependent strength of the middle and lower crust is based on the Von Mises failure criterion:

$$K_\phi = \frac{2}{\sqrt{3}}\sigma_C$$
$$\sigma_c = \left[\left(\frac{\dot{\varepsilon}}{A f_{H_2O}}\right) EXP\left(\frac{Q}{RT}\right)\right]^{\frac{1}{n}} \tag{4}$$

where K_ϕ is the shear strength of the material, $\dot{\varepsilon}$ is the shear strain rate, A is the pre-exponential constant, f_{H_2O} is the water fugacity, Q is the activation energy, R is the gas constant, T is the temperature (K) and n is the stress exponent. Temperature-dependent weakening is modeled by decreasing the value of K_ϕ with increasing temperature broadly consistent with yield stress data for wet quartzite (Hirth et al., 2001). The post-failure flow law for both the upper and lower crust is a linear viscous relationship in which the viscosity is a function of K_ϕ.

In addition to the plastic lithosphere, we define an elastic backstop that is fixed in space, representing strong cratonic lithosphere (e.g., Koons, 1990; Willett et al., 1993; Koons et al., 2002; Upton et al., 2003). We also define material properties of the subducting lithosphere based on flow law data of olivine (Kohlstedt et al., 1995), representing a subducting oceanic lithosphere. The strength of the asthenosphere in the slab window is negligible and is described by the flow strength of olivine at 1300 °C (Hirth and Kohlstedt, 1996). Kinematic boundary conditions are prescribed with a fixed velocity along the base of the subducing lithosphere (10 km/my) and fixed velocity conditions in the cratonic backstop (0 km/my). Velocities away from the boundaries are free to change as a function of far-field boundary kinematics (e.g., Koons et al., 2002; Upton et al., 2003; Johnson et al., 2004; Beaumont et al., 2004).

Due to uncertainties in the behavior and description of the lower crust in the models, the results presented in this paper are only truly

applicable for the behavior of the middle and upper crust, which is the typical crustal level exposed in ancient slab window environments (e.g. Royoke Belt Japan (Brown, 1998; Iwamora, 2000); Leech River Complex (Rusmore and Cowan, 1985; Groome et al., 2003)).

5. Numerical models

5.1. Thermal model results

Due to low convergence rates in our models, the temperatures encountered in the models are considered to be maximums and not typical for slab window environments. However, we consider the pattern of heating and cooling within a slab window environment to be more illustrative of the effects of slab window migration than the absolute temperatures attained in the model; therefore, despite the relatively high temperatures in our models, the pattern and history of heating and cooling is illustrative for natural slab window environments.

Oblique collision of the spreading ridge results in subduction zone-parallel migration of the triple junction, and the resultant slab window. The rate of margin-parallel migration will determine the advective heat transfer rate along the leading edge of the slab window as well as the duration of heating directly above the slab window — slow migration velocities lead to slower advective heat transfer and protracted heating whereas fast migration velocities lead to faster advective heat transfer and shorter heating times. In the thermal model presented here, the triple junction migrates at a rate of 10 km/my parallel to the subduction zone (Figs. 3 and 4). This results in an asymmetric thermal structure on either side of the slab window because the migration rate is faster than the conductive cooling/heating rate. Along the leading edge of the slab window, compressed isotherms in the overriding lithosphere develop as a result of high Peclet Number heat transfer (i.e., advection>conduction) (Fig. 4). Faster triple junction migration rates should enhance the asymmetrical pattern in our models because the migration rate will be that much faster than conductive heating rates.

Thermal cross-sections perpendicular to the subduction zone, and thermal histories at locations 50, 150 and 250 km from the plate margin, reveal the vertical thermal structure of the orogen (Fig. 3). Perpendicular to the subduction zone, the thermal structure is a function of the proximity to the slab window, which in our model can be used as a proxy for the time before and after slab window migration because of our simple plate-parallel migration of the triple junction (i.e., a cross-section 40 km ahead of the triple junction illustrates the thermal structure 4 million years before the triple junction reaches that point). Thermal sections in front of the triple junction illustrate progressive heating of the orogen as the slab window migrates beneath it. Distal to the triple junction (+60 km section), the thermal effects of the slab window have not been felt and the thermal structure is similar to the pre-slab window steady state.

Thermal sections along the trailing edge of the slab window record the progressive thermal relaxation after the migration of the slab window. Thermal relaxation is manifest in two ways: 1) cooling in the outboard region occurs because the rapid heating associated with the passage of the slab window does not allow for long-term heating of the outboard region and the rapid migration of cooler subducting lithosphere serves to cool the outboard region quickly, and 2) heating in the intervening region occurs because asthenospheric heating has occurred for long enough for conductive heat transfer to occur. Diachronous heating from outboard to inboard regions suggests that metamorphism associated with ridge subduction should be diachronous in the orogen.

Horizontal sections through the model (i.e., map views) reveal the thermal structure of the orogen in the third dimension (Fig. 4). Subduction zone-parallel migration of the slab window leads to the deflection of isotherms towards the trailing edge of the slab window. This occurs because the slab window migrates faster than conductive heat transfer can occur along the leading edge of the plate (i.e., it is a high Peclet Number regime) whereas regions along the trailing edge of the slab window have experienced protracted heating and experience slower conductive cooling after the passage of the slab window (i.e., it is a low Peclet Number regime). The deflection of the isotherms indicates that there may be a lag time between the passage of the triple junction at the plate boundary and metamorphism in the forearc region. The lag time between triple junction migration and heating in the forearc will be a function of triple junction migration rate and the orientation of the slab window margin.

The thermal evolution of a slab window environment has natural consequences for the metamorphic evolution of a forearc setting. Using a simplified petrogenetic grid for pelitic rocks (e.g., Bucher and Frey, 1994) one can see how the thermal effects of slab window migration may affect the metamorphic evolution of an orogen, which in most cases is the only available proxy for the thermal state of a region (Fig. 5). The main assumptions in this treatment are: 1) metamorphic facies reflect the maximum temperatures attained in a region, 2) reactions occur at the equilibrium temperature rather than at an overstepped temperature, and 3) metamorphic facies are generalized. It can be seen that maximum metamorphic grades are associated with the passage of the slab window, and that metamorphism is diachronous along strike of the orogen, with lower temperature metamorphic facies distal to the slab window contemporary with high-temperature facies proximal to the slab window. The time that a region remains at elevated metamorphic grades is a function of the residence time of the slab window, with regions over the wider part of the slab window experiencing more protracted reaction times than regions above narrower parts of the slab window. For this reason, further inboard regions will experience more protracted periods of metamorphism than outboard regions, but because the inboard regions are vertically more separated from the upwelling asthenosphere they experience lower maximum temperatures than those closer to the trench.

5.2. Mechanical models

One mechanical model is presented in this paper, with orthogonal plate convergence ($V_x = V_{total}$, $V_y = 0$). The model results provide an end-member scenario in which the triple junction remains stationary through time, but does provide valuable information about possible mechanical manifestations of slab window environments. Model results are displayed in terms of velocity components and average strain rate

$$\dot{\varepsilon}_{i,j} = \frac{1}{2}\left(\frac{\partial v_j}{\partial_i} + \frac{\partial v_i}{\partial_j}\right) \tag{5}$$

where $\dot{\varepsilon}_{ij}$ is the shear strain rate, v_i is the velocity component in the i direction and v_j is the velocity component in the j direction.

In this model, we pre-determine the amount of weakening above the slab window as a function of the thermal state of the overriding lithospheric plate, as determined previously. Vertical migration of the brittle–ductile transition is the most obvious mechanical manifestation of slab window-related thermal weakening. In the continental crust, the brittle–ductile transition is typically considered to be approximately the 350 °C isotherm, the temperature at which ductile deformation mechanisms require less shear stress than brittle deformation in quartzites (e.g., Hirth and Kohlstedt, 1996; Hirth et al., 2001). In Fig. 6, cross-sections perpendicular to the subduction zone show the depth to the 350 °C isotherm in our models, which we take as the brittle–ductile transition.

Orthogonal convergence between the two plates without a slab window results in the development of a two-sided orogenic wedge, similar to those described elsewhere (e.g., Koons, 1990; Willett et al., 1993; Beaumont et al., 1996; Fig. 7, +400 km section). High vertical velocities are present in both the outboard and inboard regions of the

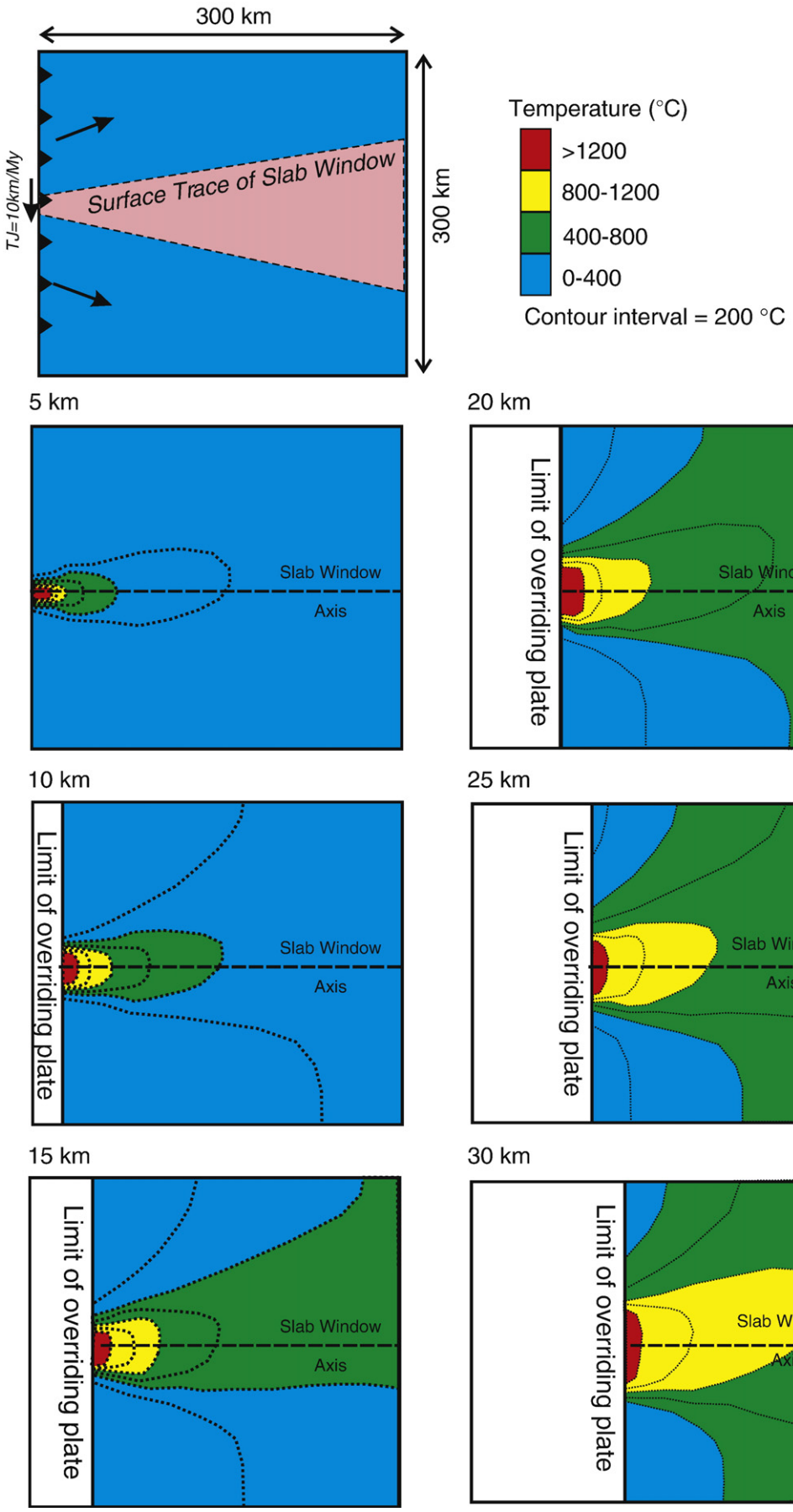

Fig. 4. Map views of the instantaneous thermal structure of the model at various depths within the model. Contour intervals are the same as on Fig. 3 for comparison.

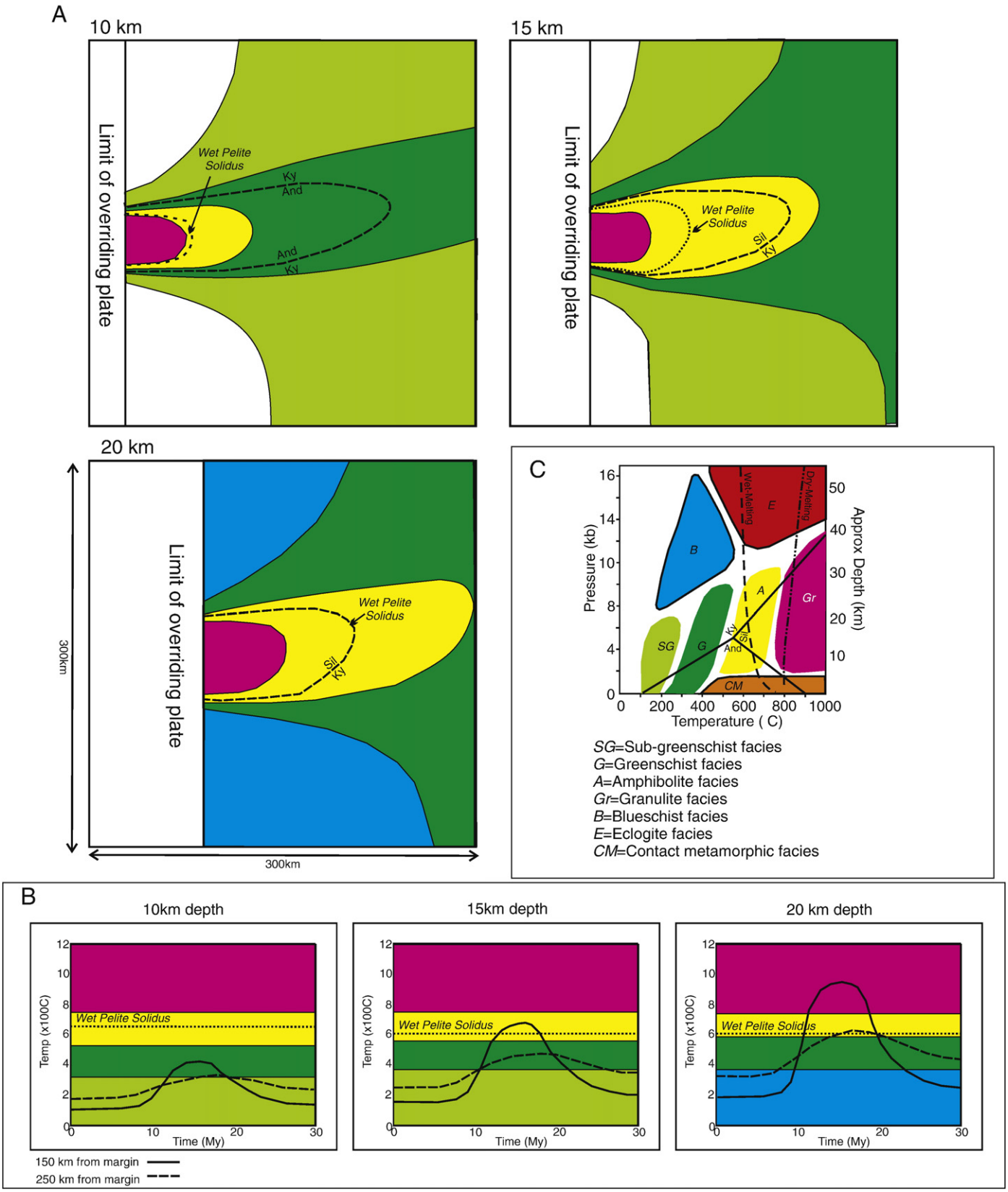

Fig. 5. A: Instantaneous metamorphic facies distribution maps for 10, 15 and 20 km depths in the model and B: metamorphic histories at points 150 and 250 km from the plate margin (the same points as in Fig. 3). C: Metamorphic facies are idealized based on pelitic bulk compositions and both the maps and histories assume that metamorphism is instantaneous and that the crust is fertile for appropriate reactions. Slab window migration is from top to bottom on each map.

orogen. Orogen-bounding shear zones form at the outboard and inboard toes of the orogen, recording a different sense of shear from outboard to inboard.

Weakening above the slab window leads to the development of a zone with greater vertical velocity in the outboard region relative to regions above normal subduction, without the added effect of

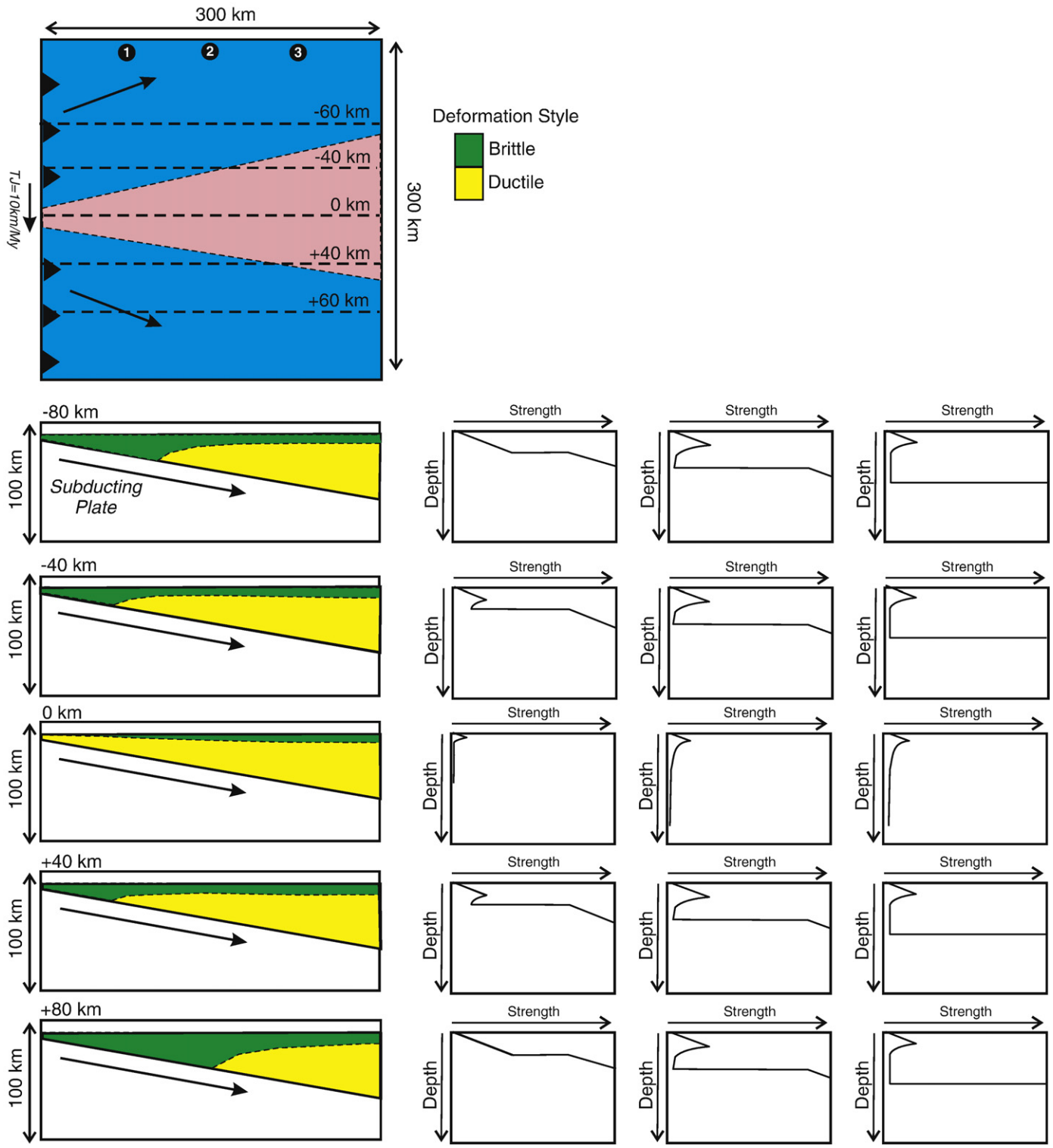

Fig. 6. Cross-sections showing the depth to the brittle–ductile transition based on the thermal model results and lithospheric strength profiles for the models. The brittle–ductile transition is shown as the 350 °C isotherm. Strength profiles are representative of lithospheric sections 50, 150 and 250 km from the plate margin.

decreased density due to heating (Fig. 7, 0 km section). Changes in asthenospheric velocity vectors above the slab window, due to changes in asthenosphere flow, result in changes in the magnitude of uplift, but an enhanced uplift zone develops above the slab window. Enhanced uplift zones above the weakened lithosphere are consistent with analytical treatments of critical wedge dynamics (e.g., Davis et al., 1983; Dahlen, 1984) and numerical models investigating the effects of lithospheric weakening via partial melting (e.g., Beaumont et al., 2004; Groome et al., 2008) and changes in basal traction (e.g., Upton et al., 2003). Lithospheric weakening also affects the localization

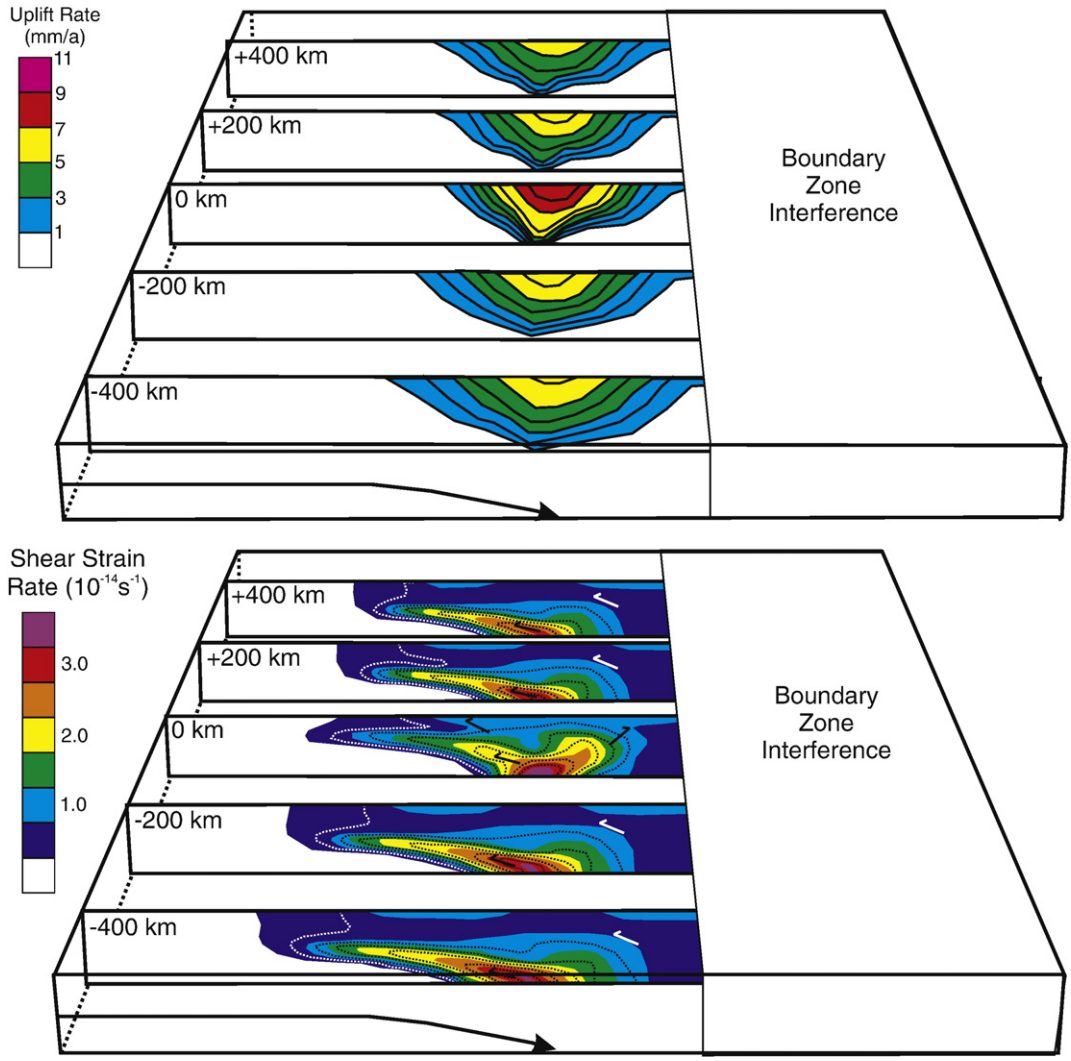

Fig. 7. Stacked cross-sections of the vertical velocity (top) and shear strain rate (bottom) for the model with orthogonal plate convergence ($V_x = V_{total}$, $V_y = 0$). The area of boundary zone interference (i.e. unreliable results) is covered by the white boxes. Note that both high uplift rates and elevated strain rates are associated with the centre of the slab window, where thermal weakening is most pronounced (see Fig. 6).

of high strain-rate zones, with high strain-rate zones localizing in the weakened zones in response to the formation of enhanced uplift zones (Fig. 7, 0 km section).

6. Discussion

The models presented above make certain predictions that can be tested by looking at regions affected by slab window migration. Among these are: 1) slab window migration heats the outboard part of the continental margin, leading to high-temperature metamorphism in the forearc; 2) slab window migration weakens the overriding lithosphere along the trailing edge of the window but not along the leading edge, which should result in different deformation styles in front of and behind the slab window; and 3) weakening behind the slab window allows for rapid vertical motions in the orogen, which should result in the formation of topographic plateaus behind the slab window. Factors not accounted for in our models, but may significantly affect the dynamics of the orogen, include: 1) erosion; 2) density differences between crust, lithospheric mantle and asthenospheric mantle; and 3) the mechanical models are not coupled with the thermal models, so thermal advection associated with the velocity field in the orogen is neglected. Below, we first qualitatively address the possible effects of factors not accounted for in our models, and then compare our model results with observations from natural examples.

6.1. Factors not accounted for

6.1.1. The effects of erosion

Because we are not modeling a particular orogen, we did not wish to impose an arbitrary erosive regime. We can, however, make the following generalities: 1) focused or orographic erosion will lead to further lithosphere weakening in the region of high uplift associated with the slab window, and 2) enhanced uplift will be associated with enhanced erosion and exhumation unless it is an arid environment. These generalities will also affect our comparison between the model results and natural examples, although the topographic uplift in our models is transient and may not be well represented in the geologic record.

6.1.2. The effects of density variations

The replacement of cold lithospheric mantle with hot asthenospheric mantle changes the isostatic balance above a slab window. Upwelling buoyant asthenosphere in the slab window may result in isostatic uplift of the overriding plate above the slab window, leading to the

development of topographic highs above the slab window (e.g., Wong and Wortel, 1997; Buiter et al., 2002; Rogers et al., 2002). In Central America, a plateau above the inferred location of the Cocos–Nazca slab window correlates with a low velocity zone in the mantle that has been interpreted to be a location of asthenospheric upwelling (e.g., Rogers et al., 2002). Epiorogenic uplift of the Central American highlands above the zone of asthenospheric upwelling was attributed by Rogers et al. (2002) to changes in isostatic balance associated with heating above the asthenosphere. Numerical modeling (e.g., Buiter et al., 2002) show that the replacement of cold lithospheric mantle by hot asthenospheric mantle can result in topographic uplift by changes in isostatic balance. In our models, we do not account for a buoyant asthenospheric mantle in the slab window, nor do we account for reductions in density in the overriding lithosphere along the trailing edge of the slab window resulting from heating. Based on observations and models of the surface effects of asthenospheric upwelling (e.g., Rogers et al., 2002; Buiter et al., 2002) we can hypothesize that a reduction in mantle density within the slab window should add an isostatic uplift to the mechanically-induced uplift we see in our models.

6.2. Comparison with natural examples

6.2.1. High-temperature metamorphism and magmatism in the forearc region

Perhaps the most-studied example of forearc metamorphism and magmatism attributed to slab window migration is the Cretaceous–Paleogene forearc of the northern Cordillera (British Columbia and Alaska) (e.g., Hill et al., 1981; Barker et al., 1992; Sisson and Pavlis, 1993; Haeussler et al., 1995; Harris et al., 1996; Groome et al., 2003; Sisson et al., 2003; Pavlis and Sisson, 2003). This exhumed forearc belt records widespread high-temperature metamorphism and associated magmatism ranging in age from 80 to 40 Ma (e.g., Barker et al., 1992; Haussler et al., 1995; Sisson and Pavlis, 1993; Groome et al., 2003; Sisson et al., 2003) that in some places overprints an earlier record of high-pressure metamorphism (e.g., Fairchild and Cowan, 1982; Rusmore and Cowan, 1985; Groome et al., 2003). Igneous rocks in this belt record complex mixing relationships including MORB and crustal components that has been interpreted to represent mixing between asthenosphere- and crustally-derived partial melts (e.g., Rogers and Saunders, 1989; Barker et al., 1992; Harris et al., 1996; Bradley et al., 2003; Groome et al., 2003; Sisson et al., 2003).

The high-temperature metamorphic record in this forearc belt is consistently in the andalusite–sillimanite stability field, and locally includes migmatites (e.g., Fairchild and Cowan, 1982; Groome et al., 2003; Sisson et al., 2003; Zumsteg et al., 2003). This record contrasts with typical forearc metamorphic signatures, which are generally in the kyanite stability field and locally blueschist facies (e.g., Bucher and Frey, 1994). In some cases, the high-temperature metamorphic units are localized around syn-tectonic felsic intrusions (e.g., Groome et al., 2003), but in many cases the extent of high-temperature metamorphism is more widespread, suggesting a regional heat source (e.g., Sisson et al., 2003). At the southernmost extent of the Cretaceous–Paleogene forearc belt, on southern Vancouver Island, high-temperature metamorphism is younger than high-pressure metamorphism in time-correlative tectonostratigraphic units in relatively close proximity (e.g., Rusmore and Cowan, 1985; Brandon et al., 1989; Groome et al., 2003). Jurassic–Cretaceous high-pressure metamorphism in the blueschist facies is recorded in the Pandora Peak Unit of the Leech River Complex and the Pacific Rim Complex of the Pacific Rim Terrane (e.g., Rusmore and Cowan, 1985; Brandon et al., 1989). Eocene high-temperature metamorphism (in the andalusite stability field) in the Leech River Schist unit of the Leech River Complex occurs less than 50 km along strike from the Pandora Peak Unit and is associated with a contemporaneous felsic dyke swarm (e.g., Fairchild and Cowan, 1982; Groome et al., 2003).

Brown 1998 hypothesized that the synchronous development of high- and low-temperature metamorphic belts in Japan (Ryoke and Sanbagawa belts) are the manifestation of ridge subduction. By this model, heating in the vicinity of the subducting ridge results in the development of the high-temperature metamorphic belt, whereas the low-temperature metamorphic belt develops in regions where ridge subduction does not occur (e.g., Brown, 1998; Iwamora, 2000). In Japan, the development of these metamorphic belts is associated with the formation of a large granitic batholith, and there may be a relationship between granite intrusion and the formation of the high-temperature metamorphic belt (e.g., Lux et al., 1986; Barton and Hanson, 1989; Iwamora, 2000), but Iwamora (2000) hypothesized that the underlying heat source for batholith formation may be from ridge subduction.

Heat flow in South America is highest above the inferred location of the Chile Ridge slab window (e.g. Hamza and Munoz, 1996; Murdie and Russo, 1999), possibly indicating an asthenospheric heat source in this region. Heat flow in the Andes varies along strike from approximately 78 mW m^{-2} in the north to approximately 160 mW m^{-2} in the Patagonia region (Hamza and Munoz, 1996). Murdie and Russo (1999) also recorded high heat flow measurements in the Patagonian region in shallow lake sediments. Assuming an average thermal conductivity of approximately 3 W m^{-1} K^{-1} (e.g. Turcotte and Schubert, 2002) and no internal heat generation, these heat flow values indicate a near-surface steady-state geothermal gradient of approximately 50 °C/km in the Patagonian region, compared with 25 °C/km farther north in the Andes, which if extrapolated to greater depths should result in low-pressure, high-temperature metamorphism in the Patagonian region. High heat flow values in the Patagonian region are spatially coincident with the location of the inferred Nazca–Antarctica slab window beneath South America, suggesting a causative relationship.

Model results compare well with natural examples. Due to low convergence rates and elevated initial temperatures in our models, the absolute temperatures in the models should not be viewed as representative of the conditions expected in nature, rather it is the pattern of transient heating and cooling that is important in these models.

In regions unaffected by the slab window, *P–T* conditions are in the high-pressure, low-temperature stability field, typical of forearc settings (Fig. 5). This should lead to high-pressure metamorphism. However, in regions above the migrating slab window, *P–T* conditions are towards the high-temperature field, which should result in high-temperature metamorphism in the forearc, potentially in the partial melting stability range (Fig. 5). When viewed as a temporal evolution, any given point in the forearc should record an early low-temperature metamorphism overprinted by a high-temperature metamorphism, as seen in many regions affected by slab windows.

Immediately above the slab window, geotherms are highly variable depending on the depth to the upwelling asthenosphere. Geothermal gradients are up to 100 °C/km where the asthenosphere is shallowest and typically on the order of 40–50 °C/km in the slab window environment. This compares with 15–20 °C/km in regions unaffected by slab window migration. Regardless of the absolute temperatures, the pattern of high geothermal gradients in the slab window environment relative to regions outside the slab window region is illustrative of what occurs in natural settings.

6.2.2. Changes in deformation kinematics during slab window migration

The Cretaceous–Paleogene forearc of the northern Cordillera also provides insight into changes in deformation kinematics associated with slab window migration (e.g., Bradley et al., 2003; Pavlis and Sisson, 2003). Plate convergence vectors for the Kula and Farallon plates record different magnitudes of subduction zone-parallel motion (e.g., Engebretson et al., 1985), which should result in changes in the magnitude of transpressional deformation in the overriding plate as the slab window migrated along the margin. Changes in deformation kinematics from contractional to transpressional in the forearc are explained by changes in convergence vectors, with later Kula Plate vectors being more oblique than earlier Farallon Plate (or

Resurrection Plate) vectors (e.g., Engebretson et al., 1985; Sisson and Pavlis, 1993; Haeussler et al., 2003; Pavlis and Sisson, 2003; Roeske et al., 2003). Haeussler et al. (2003) detailed this change in kinematics by investigating brittle structures in the Gulf of Alaska region, noting that there was an early stage of margin-normal contraction, attributed to subduction of the Farallon Plate, overprinted by margin-parallel extension, attributed to passage of the slab window, finally overprinted by dextral strike-slip faulting, attributed to subduction of the Kula Plate. Similar overprinting relationships have been noted in higher-grade metamorphic rocks in the Alaska forearc (e.g. Sisson and Pavlis, 1993; Pavlis and Sisson, 2003; Roeske et al., 2003).

Subduction of the Chile Ridge beneath the Patagonian Andes resulted in a Nazca–Antarctic slab window starting in the Miocene (e.g., Barker, 1982; Espinoza et al., 2005; Breitsprecher and Thorkelson, this volume). Active subduction of the Chile Ridge and active deformation in the Patagonian Andes provide an ideal setting to investigate the direct effects of slab window migration on the deformation style in the overriding plate. South America–Nazca plate convergence vectors in the Patagonian region are more oblique than South America–Antarctica plate convergence vectors (e.g., Legabrielle et al., 2004; Espinoza et al., 2005; Breitsprecher and Thorkelson, this volume). This resulted in the northward migration of the Chile Ridge since the Miocene. Based on the plate convergence vectors, deformation associated with the passage of the Chile Ridge should record early dextral transpression (associated with Nazca Plate subduction) overprinted by contraction-dominated deformation (associated with Antarctic Plate subduction).

Indeed, early deformation in the Patagonian fold and thrust belt is predominantly dextral transpressive and is overprinted by compressive deformation, including significant uplift (e.g., Suarez et al., 2000; Cembrano et al., 2002; Legabrielle et al., 2004; Espinoza et al., 2005). The timing and orientation of early and late structures are consistent with changes from Nazca to Antarctic subduction (e.g., Legabrielle et al., 2004). In regions believed to be above the asthenospheric window, deformation is dominantly extensional, which could be attributed to either divergent velocities in the asthenosphere being transmitted to the overriding lithosphere or upwelling of the asthenosphere resulting in isostatic uplift-induced extension — i.e., gravitational spreading.

Changes in deformation style during the passage of a slab window in both the ancient northern Cordillera forearc and the active Patagonian region have been attributed to changes in plate convergence vectors from one plate to the other. However, it is possible that thermal weakening of the overriding lithosphere above the slab window could also have an effect on the change in deformation style, as seen in the models presented here. Pavlis and Sisson, (2003) recognized a significant change in rheologic behaviour in the core of the Chugach Complex in Alaska at the contact between amphibolite-facies gneisses and amhibolite-greenschist-facies schists that they attribute to the passage of the slab window. Early flat-lying, localized shear zones recording dextral shear sense predate peak metamorphism in the Chugach Complex and have been attributed to oblique subduction of the Farallon Plate accompanied by vertical shortening (e.g., Pavlis et al., 2003). These flat-lying structures are overprinted by more distributed, steeper-dipping structures associated with peak metamorphism (e.g., Pavlis et al., 2003). Pavlis et al. (2003) identified two possible causes for this change in deformation style: 1) upward migration of the thermal front that caused the prograde metamorphism, and 2) a change from Farallon Plate to Kula Plate subduction leading to a change in deformation kinematics. These are not necessarily mutually-exclusive models because the transition from one plate to the other involved the passage of the slab window, which would have heated the lithosphere from below such that the change in deformation style did not occur until the thermal pulse conducted through the lithosphere, allowing it to weaken.

In our models, the convergent kinematics on either side of the slab window are the same, so we cannot test the changes in deformation kinematics related to changes in boundary conditions, but this is a reasonable interpretation. What our models do illustrate is the change in strain-rate distribution, and hence deformation histories, related to heating within the slab window. Within the slab window, where the lithosphere has experienced the most thermal weakening, strain rates are high relative to regions outside the thermally-weakened region. The elevated strain rates in this area should lead to more intense deformation as the slab window migrates, which would in turn be manifest in nature as a time period of intense ductile deformation associated with high-temperature metamorphism. This is the case in natural slab window environments, including the Leech River Complex on Vancouver Island (e.g., Groome et al., 2003) and the Chugach Complex in Alaska (e.g., Pavlis and Sisson, 2003).

6.2.3. Enhanced uplift associated with slab windows

The Cretaceous–Paleogene forearc of the northern Cordillera also provides some insight into uplift and exhumation rates associated with slab window migration. In the southern part of this belt (Vancouver Island), rapid post-thermal peak exhumation is recorded in the Leech River Complex (e.g., Groome et al., 2003). In the Leech River Complex, peak metamorphism was andalusite–staurolite grade ($P<3$ kb, $T\sim550$ °C) and was accompanied by emplacement of a felsic dyke swarm at approximately 51 Ma (Groome et al., 2003). Rapid cooling is indicated by progressive cooling ages from muscovite (~45 Ma) and biotite (~42 Ma), resulting in a cooling rate of approximately 29 C/my (Groome et al., 2003). Final exhumation of the Leech River Complex is constrained by the presence of unmetamorphosed clastic sediments, which locally include clasts of Leech River schist, overlying the complex that has been constrained to be Oligocene based on fossils (e.g., Fairchild and Cowan, 1982), resulting in a minimum exhumation rate of 0.8 km/my. Groome et al. (2003) attributed the rapid exhumation of the Leech River Complex to tectonic wedging between the accreting Crescent Terrane and the older Wrangell Terrane, although the thermal weakening associated with slab window migration is likely to have played a role.

Modern examples also record evidence for rapid topographic uplift associated with the passage of a subducting ridge. In Central America, the Central American Plateau is a large region of >1000 m elevation in the backarc region of the active arc. The volcanic arc in this region records anomalous geochemical signatures (i.e. an asthenospheric component mixed with "typical" arc magmas) suggesting the presence of a slab window beneath the arc (e.g., Johnston and Thorkelson, 1997). P-wave mantle tomography in this region revealed the presence of a region of low seismic velocities, interpreted to be hot asthenosphere, at depth below the backarc plateau (Rogers et al., 2002) and uplift in the plateau has been attributed to changes in isostatic balance associated with the replacement of cold, dense lithosphere by hot, buoyant asthenosphere (Rogers et al., 2002). Numerical models of slab break-off, resulting in the replacement of lithospheric mantle with asthenospheric mantle indicate that rapid uplifts should be recorded at the surface above the upwelling asthenosphere (e.g., Wong and Wortel, 1997; Van de Zedde and Wortel, 2001; Buiter et al., 2002) because the isostatic balance is changed. The mechanism of lithospheric replacement in these models is different than what occurs in a slab window, but the effects should be similar.

In the Patagonian Andes, rapid topographic uplift is associated with the subduction of the Chile Ridge (e.g., Legabrielle et al., 2004). In this region, uplift is associated with deformation in the fold-thrust belt, not isostatic uplift above the buoyant asthenospheric window (e.g., Suarez et al., 2000; Legabrielle et al., 2004). Uplift and contractional deformation in this region has been attributed to changes in plate convergence vectors (e.g., Legabrielle et al., 2004), although the effects of thermal weakening above the slab window are also plausible.

Elevated uplift rates in the forearc of our models are shown on Fig. 7a where uplift rates are significantly higher above the subducting ridge than along the periphery. In the model presented here, elevated uplift is associated with strain localization due to thermal weakening,

but the subduction of a topographic high, such as a spreading ridge, will also lead to elevated uplift rates (e.g., Dominguez et al., 2000). When coupled with erosion, elevated uplift could lead to elevated exhumation rates as seen in natural examples.

7. Conclusions

Simplified three-dimensional numerical models generally support geologic interpretations of slab window migration, including: 1) changes in deformation kinematics as the slab window migrates, 2) anomalously high-temperature metamorphism in the forearc region and 3) the generation of crustally-derived magmatism mixed with asthenosphere-derived magma in the forearc region. To these, we would add that rapid exhumation in the forearc region should also be considered a manifestation of ridge subduction for two primary reasons: 1) subduction of a topographic high should cause the trench region to be uplifted and 2) thermal weakening associated with slab window migration should facilitate rapid uplifts along the trailing edge of the slab window, and lead to rapid exhumation rates of high-grade metamorphic rocks.

Important new insights provided by our models include the interaction between thermal weakening above the migrating slab window and strain localization and the long thermal decay time along the trailing edge of the slab window. These have implications for the evolving deformation style in a slab window environment including the overprinting of localized (possibly brittle) deformation by more homogeneous ductile deformation in the weakened orogen. Long thermal decay times along the trailing edge of the slab window suggest that metamorphism in the forearc region is likely to be protracted because the overriding lithosphere remains at elevated temperatures after the passage of the triple junction. Protracted heating, accompanied by deformation in the thermally-weakened orogen should result in syn-kinematic metamorphism *after* the passage of the triple junction.

Although our models are simple relative to natural situations, they demonstrate fundamental relationships among the processes of heating, deformation and slab window migration. More detailed models are likely to clarify these relationships and address outstanding issues such as the effects of fluid flow on heating and metamorphism in the crust, and the thermal effects of melting of the downgoing slabs along the margins of the slab window.

Acknowledgements

Phaedra Upton and Terry Pavlis provided constructive reviews that improved this manuscript significantly.

References

Barker, P.F., 1982. The Cenozoic subduction history of the Pacific margin of the Antarctic Peninsula: ridge crest–trench interactions. Journal of the Geological Society, London 139, 787–801.

Barker, F., Farmer, G.L., Ayuso, R.A., Plafker, G., Lull, J.S., 1992. The 50 Ma granodiorite of the eastern Gulf of Alaska: melting in an accretionary prism in the forearc. Journal of Geophysical Research 97, 6757–6778.

Barton, M.D., Hanson, R.B., 1989. Magmatism and the development of low pressure metamorphic belts: implications from the Western United States and thermal modeling. GSA Bulletin 101, 1051–1065.

Beaumont, C., Kamp, P.J.J., Hamilton, J., Fullsack, P., 1996. The continental collision zone, South Island, New Zealand: comparison of geodynamical models and observations. Journal of Geophysical Research 101, 3333–3360.

Beaumont, C., Jamieson, R.A., Nguyen, M.H., Medvedev, S., 2004. Crustal channel flows: 1. Numerical models with applications to the tectonics of the Himalayan–Tibetan orogen. Journal of Geophysical Research 109. doi:10.1029/2003JB002809.

Bradley, D., Kusky, T., Haeussler, P., Goldfarb, R., Miller, M., Dumoulin, J., Nelson, S.W., Karl, S., 2003. Geologic signature of early Tertiary ridge subduction in Alaska. In: Sisson, V.B., Roeske, S.M., Pavlis, T.L. (Eds.), Orogen Developed During Ridge–Trench Interaction Along the North Pacific Margin, GSA Special Paper. Geology of a Transpressional, vol. 371, pp. 19–50.

Brandon, M.T., 1989. Deformational styles in a sequence of olistostromal mélanges, Pacific Rim Complex, western Vancouver Island. GSA Bulletin 101, 1520–1542.

Breitsprecher, K., Thorkelson, D.J., Groome, W.G., Dostal, J., 2003. Geochemical confirmation of the Kula–Farallon slab window beneath the Pacific Northwest in Eocene time. Geology 31, 351–354.

Brown, M., 1998. Ridge–trench interactions and high-T–low-P metamorphism, with particular reference to the Cretaceous evolution of the Japanese Islands. In: Treloar, P.J., O'Brien, P.J. (Eds.), What Drives Metamorphism and Metamorphic Reactions. Geological Society Special Publication, vol. 138, pp. 131–163.

Bucher, K., Frey, M., 1994. Petrogenesis of Metamorphic Rocks, (6th Ed). Springer Verlag, Berlin. 318 p.

Buiter, S., Govers, R., Wortel, M.J.R., 2002. Two-dimensional simulations of surface deformation caused by slab detachment. Tectonophysics 354, 195–210.

Cembrano, J., Lavenu, A., Reynolds, P., Arancibia, G., Lopez, G., Sanhueza, A., 2002. Late Cenozoic transpressional ductile deformation north of the Nazca–South America–Antarctica triple junction. Tectonophysics 354, 289–314.

Dahlen, F.A., 1984. Noncohesive critical coulomb wedges: an exact solution. Journal of Geophysical Research 89, 10125–10133.

Davis, D., Suppe, J., Dahlen, F.A., 1983. Mechanics of fold-and-thrust belts and accretionary wedges. Journal of Geophysical Research 88, 1153–1172.

Delong, S.E., Schwarz, W.M., Anderson, R.N., 1979. Thermal effects of ridge subduction. Earth and Planetary Science Letters 44, 239–246.

Dickinson, W.R., Snyder, W.S., 1979. Geometry of triple junctions related to the San Andreas transform. Journal of Geophysical Research 84, 561–572.

Dominguez, S., Malavielle, J., Lallemand, S.E., 2000. Deformation of accretionary wedges in response to seamount subduction: insights from sandbox experiments. Tectonics 19, 182–196.

Ellis, S., Beaumont, C., 1999. Models of convergent boundary tectonics: implications for the interpretation of LITHOPROBE data. Canadian Journal of Earth Sciences 36, 1711–1741.

Engebretson, D.C., Cox, A., Gordon, R.G., 1985. Relative motions between oceanic and continental plates in the Pacific Basin. GSA Special Paper 206. 59 pp.

Espinoza, F., Suarez, M., Lagabrielle, Y., Morata, D., Polve, M., Barbero, L., Maury, R., Guivel, C., De la Cruz, R., 2005. Tectonics of the Central Patagonian Cordillera related to Mio-Pliocene subduction of the Chile Ridge: preliminary morphological, chronological and geochemical evidences. 6th International Symposium on Andean Geodynamics (ISAG 2005) Extended Abstracts, pp. 250–253.

Fairchild, L.H., Cowan, D.S., 1982. Structure, petrology and tectonic history of the Leech River Complex northwest of Victoria, Vancouver Island. Canadian Journal of Earth Sciences 19, 1817–1835.

Forsythe, R.D., Nelson, E.P., 1985. Geological manifestations of ridge collision: evidence from the Golfo de Penas–Taitao Bain, southern Chile. Tectonics 4, 477–495.

Groome, W.G., Thorkelson, D.J., Friedman, R.M., Mortensen, J.K., Massey, N.W.D., Marshall, D.D., Layer, P.W., 2003. Magmatism and tectonic history of the Leech River Complex, Vancouver Island: evidence for ridge–trench intersection and accretion of the Crescent Terrane. In: Sisson, V.B., Roeske, S.M., Pavlis, T.L. (Eds.), Geology of a Transpressional Orogen Developed During Ridge–Trench Interaction Along the North Pacific Margin. GSA Special Paper, vol. 371, pp. 327–353.

Groome, W.G., Koons, P.O., Johnson, S.E., 2008. Metamorphism, transient mid-crustal rheology, strain localization and the exhumation of high-grade metamorphic rocks. Tectonics 27. doi:10.1029/2006TC001992.

Haeussler, P.J., Bradley, D., Goldfarb, R., Snee, L., Taylor, C., 1995. Link between ridge subduction and gold mineralization in southern Alaska. Geology 23, 995–998.

Haeussler, P.J., Bradley, D.C., Goldfarb, R.J., 2003. Brittle deformation along the Gulf of Alaska margin in response to Paleocene–Eocene triple junction migration. In: Sisson, V.B., Roeske, S.M., Pavlis, T.L. (Eds.), Geology of a Transpressional Orogen Developed During Ridge–Trench Interaction Along the North Pacific Margin. GSA Special Paper, vol. 371, pp. 119–140.

Hamza, V.M., Munoz, M., 1996. Heat flow map of South America. Geothemics 25, 599–646.

Harris, N.R., Sisson, V.B., Wright, J.E., Pavlis, T.L., 1996. Evidence for Eocene mafic underplating during forearc intrusive activity, eastern Chugach Mountains, Alaska. Geology 24, 263–266.

Hibbard, J.P., Laughland, M.M., Kang, S.M., Karig, D., 1993. The thermal imprint of spreading ridge subduction on the upper structural levels of an accretionary prism, southwest Japan. In: Underwood, M.B. (Ed.), Thermal Evolution of the Tertiary Shimanto Belt, Southwest Japan: An Example of Ridge–Trench Interaction. GSA Special Paper, vol. 273, pp. 83–102.

Hill, M., Morris, J., Whelan, J., 1981. Hybrid granodiorites intruding the accretionary prism, Kodiak, Shumagin and Sanak Islands, Southwest Alaska. Journal of Geophysical Research 86, 10569–10590.

Hirth, G., Kohlstedt, D.L., 1996. Water in the oceanic upper mantle: implications for rheology, melt extraction and the evolution of the lithosphere. Earth and Planetary Science Letters 144, 93–108.

Hirth, G., Tessier, C., Dunlap, W., 2001. An evaluation of quartzite flow laws based on comparisons between experimentally and naturally deformed rocks. International Journal of Earth Sciences 90, 77–87.

Itasca Consulting Group, Inc, 2005. FLAC 3D (Fast Lagrangian Analysis of Continua in 3 Dimensions) Version 3.0.

Iwamora, H., 2000. Thermal effects of ridge subduction and its implications for the origin of granitic batholiths and paired metamorphic belts. Earth and Planetary Science Letters 181, 131–144.

Ji, S., Zhao, P., 1993. Flow laws of multiphase rocks calculated from experimental data on the constituent phases. Earth and Planetary Science Letters 117, 181–187.

Ji, S., Xia, B., 2002. Rheology of Polyphase Earth Materials. Polytechnique Press International, Montreal. 235 pp.

Johnson, S.E., Vernon, R.H., Upton, P., 2004. Foliation development and progressive strain-rate partitioning in the crystallizing carapace of a tonalite pluton:

microstructural evidence and numerical modeling. Journal of Structural Geology 26, 1845–1865.
Johnston, S.T., Thorkelson, D.J., 1997. Cocos–Nazca slab window beneath Central America. Earth and Planetary Science Letters 146, 465–474.
Kohlstedt, D.J., Evans, B., Mackwell, S.J., 1995. Strength of the lithosphere: constraints imposed by laboratory experiments. Journal of Geophysical Research 100, 17587–17602.
Koons, P.O., 1990. Two-sided orogen: collision and erosion from the sandbox to the Southern Alps, New Zealand. Geology 18, 679–682.
Koons, P.O., Zeitler, P.K., Chamberlain, C.P., Craw, D., Meltzer, A.S., 2002. Mechanical links between erosion and metamorphism in Nanga Parbat, Pakistan Himalaya. American Journal of Science 302, 749–773.
Legabrielle, Y., Suarez, M., Rossello, E.A., Herail, G., Martinod, J., Regnier, M., De la Cruz, R., 2004. Neogene to Quaternary tectonic evolution of the Patagonian Andes at the latitude of the Chile Triple Junction. Tectonophysics 385, 211–241.
Lux, D.R., DeYoreo, J.J., Guidotti, C.V., Decker, E.R., 1986. Role of plutonism in low-pressure metamorphic belt formation. Nature 323, 794–797.
Madsen, J.K., Thorkelson, D.J., Friedman, R.M., Marshall, D.D., 2005. Cenozoic to Recent plate configurations in the Pacific Basin: Ridge subduction and slab window magmatism in western North America. Geosphere 2, 11–34.
Marshak, R.S., Karig, D.E., 1977. Triple junctions as a cause for anomalously near-trench igneous activity between the trench and volcanic arc. Geology 5, 233–236.
Murdie, R.E., Russo, R.M., 1999. Seismic anisotropy in the region of the Chile margin triple junction. Journal of South American Earth Sciences 12, 261–270.
Pavlis, T.L., Sisson, V.B., 2003. Development of a subhorizontal decoupling horizon in a transpressional system, Chugach metamorphic complex, Alaska: evidence for rheological stratification f the crust. In: Sisson, V.B., Roeske, S.M., Pavlis, T.L. (Eds.), Geology of a Transpressional Orogen Developed During Ridge–Trench Interaction Along the North Pacific Margin. GSA Special Paper, vol. 371, pp. 191–216.
Roeske, S.M., Snee, L.W., Pavlis, T.L., 2003. Dextral-slip reactivation of an arc–forearc boundary during Late Cretaceous–Early Eocene oblique convergence in the northern Cordillera. In: Sisson, V.B., Roeske, S.M., Pavlis, T.L. (Eds.), Geology of a Transpressional Orogen Developed During Ridge–Trench Interaction Along the North Pacific Margin. GSA Special Paper, vol. 371, pp. 141–170.
Rogers, G., Saunders, A.D., 1989. Magnesian andesites from Mexico, Chile and the Aleutian Islands: implications for magmatism associated with ridge–trench collisions. In: Crawford, A.J. (Ed.), Boninites and Related Rocks. Unwin Hyman, London, pp. 416–445.
Rogers, R.D., Karason, H., van der Hilst, R.D., 2002. Epeirogenic uplift above a detached slab in northern Central America. Geology 30, 1031–1034.
Rusmore, M.E., Cowan, D.S., 1985. Jurassic–Cretaceous rock units along the southern edge of the Wrangellia Terrane on Vancouver Island. Canadian Journal of Earth Sciences 22, 1223–1232.
Sisson, V.B., Pavlis, T.L., 1993. Geologic consequences of plate reorganization: an example from the Eocene of southern Alaska forearc. Geology 21, 913–916.
Sisson, V.B., Poole, A.R., Harris, N.R., Cooper-Burner, H., Pavlis, T.L., Copeland, P., Donelick, R.A., McClelland, W.C., 2003. Geochemical and geochronologic constraints for genesis of a tonalite–trondhjemite suite and associated mafic intrusive rocks in the eastern Chugach Mountains, Alaska: a record of ridge-transform subduction. In: Sisson, V.B., Roeske, S.M., Pavlis, T.L. (Eds.), Geology of a Transpressional Orogen Developed During Ridge–Trench Interaction Along the North Pacific Margin. GSA Special Paper, vol. 371, pp. 293–326.
Suarez, M., De la Cruz, R., Bell, C.M., 2000. Timing and origin of deformation along the Patagonian fold and thrust belt. Geological Magazine 137, 345–353.
Thorkelson, D.J., 1996. Subduction of diverging plates and the principles of slab window formation. Tectonophyiscs 255, 47–63.
Thorkelson, D.J., Taylor, R.P., 1989. Cordilleran slab windows. Geology 17, 833–836.
Turcotte, D.L., Schubert, G., 2002. Geodynamics, Second Edition. Cambridge University Press. 456 p.
Underwood, M.B., Byrne, T., Hibbard, J.P., DiTullio, L., Laughland, M.M., 1993. The effects of ridge subduction on the thermal structure of accretionary prisms: a Tertiary example from the Shimanto Belt of Japan. In: Underwood, M.B. (Ed.), Thermal Evolution of the Tertiary Shimanto Belt, Southwest Japan: an Example of Ridge–Trench Interaction. GSA Special Paper, vol. 273, pp. 151–168.
Upton, P., Koons, P.O., Eberhart-Phillips, D., 2003. Extension and partitioning in an oblique subduction zone, New Zealand: constraints from three-dimensional numerical modeling. Tectonics 22. doi:10.1029/2002TC001431.
Van de Zedde, D.M.E., Wortel, M.J.R., 2001. Shallow slab detachment as a transient source of heat at midlithospheric depths. Tectonics 20, 868–882.
Willett, S., Beaumont, C., Fullsack, P., 1993. Mechanical model for the tectonics of doubly vergent compressional orogens. Geology 21, 371–374.
Wong, S.Y.M., Wortel, M.J.R., 1997. Slab detachment in continental collision zones: an analysis of controlling parameters. Geophysical Research Letters 24, 2095–2098.
Wortel, M.J.R., Spakman, W., 2000. Subduction and slab detachment in the Mediterranean–Carpathian region. Science 290, 1910–1917.
Zumsteg, C.L., Himmelberg, G.R., Karl, S.M., Haeussler, P.J., 2003. Metamorphism within the Chugach accretionary complex on southern Barnoff Island, southeastern Alaska. In: Sisson, V.B., Roeske, S.M., Pavlis, T.L. (Eds.), Geology of a Transpressional Orogen Developed During Ridge–Trench Interaction Along the North Pacific Margin. GSA Special Paper, vol. 371, pp. 253–268.